

Ellipsometric detection of optically and electron-beam induced changes in the optical properties of materials

S. A. Hadjiiski*, D. L. Lyutov, K. M. Kirilov, K. V. Genkov, G. G. Tsutsumanova, A. N. Tzonev, S. C. Russev

*Department of Solid State Physics and Microelectronics, Faculty of Physics,
St. Kliment Ohridski University of Sofia, 5 James Bourchier Blvd., BG-1164 Sofia, Bulgaria*

The main purpose of this paper is to present the results of a preliminary study of the possibility to combine two experimental methods: ellipsometry and scanning electron microscopy (SEM). Ellipsometry is a well-developed non-destructive contactless method with great sensitivity to optical properties and/or geometry of the investigated specimens in the direction perpendicular to the interface. Its lateral resolution, however, is limited by the size of the probe beam and is lesser than what could be achieved with SEM. With regard to the latter, along with the already exploited interactions (collecting secondary and/or backscattered electrons, cathodoluminescence, EDX, etc.), electron beam irradiation leads to local temperature changes and carrier injection. Ellipsometric measurement of the subsequent refractive index alteration could be used for visualization of thermal properties with micron resolution. A series of simulations were performed to study the electron beam heating effect in SEM and to estimate the optimal conditions for its optical detection. Model experiments were also conducted to confirm the results, obtained by the simulations.

Key words: ellipsometry, SEM, refractive index changes, electron beam heating, thermo-optic coefficient, carrier injection

INTRODUCTION

Ellipsometry is a well-developed method for studying the optical properties of materials by measuring changes in the polarisation of a probe beam after interaction (usually reflection) with the specimen. It is a contactless and non-destructive technique that is commonly used not only in science laboratories but in industrial facilities as well. In the context of ellipsometry a forward and inverse problem are considered. The latter involves estimating the values of some of the material properties by interpreting the measured optical response of the specimen. This is often a complex problem that has to be solved numerically, but with the contemporary computational resources and technology it is possible to conduct accurate measurements in real-time. With longitudinal resolution of 1 Å and less [1], ellipsometry can be used for high-precision control over thickness of thin films and layers. However, the signal is averaged over the entire irradiated area, so the lateral resolution is limited by the probe beam diameter. Furthermore, only a single point of the specimen is observed. It is possible to obtain a raster image of a larger area by translating the interaction spot over the specimen (scanning ellipsometry) [2]. Alternatively, a full-field image can also be achieved with imaging ellipso-

metry [1] – basically the photodetector is replaced by a CCD camera, each pixel of which is then used as a separate detector.

Significantly greater lateral resolution is inherent for SEM – top values are in the range of 1–10 nm [3]. The specimen is scanned by beam of accelerated electrons that interact with it in various ways. Some of the interactions can be used to collect data about the material [3]: topology can be observed by collecting secondary (SE) and/or backscattered electrons (BSE); elemental composition can be determined roughly by collecting BSE and more precisely with energy-dispersive (EDX) or wavelength-dispersive x-ray spectroscopy (WDX). However, there are electron-matter interactions that are still unexploited as data sources, e.g. electron-beam induced heating of the specimen [4–6] and carrier injection. Both effects result in local refractive index changes, modulated at the scanning frequency. Such alterations can be detected optically, ellipsometrically in particular.

Our work involves investigating the possibility to employ a new data source in SEM – the ellipsometric measurement of local electron-beam induced changes in the refractive index of the specimen. Although, our present investigations are focused on thermal effect modulation, they can be easily extended to carrier injection effect as well. Despite the fact that similar studies are already present (e.g. thermo- [7, 8] and

* To whom all correspondence should be sent:
shadjiiski@gmail.com

photoreflectance [9, 10], scanning electron acoustic microscopy (SEAM) [11]), the combination of SEM and ellipsometry up to our best knowledge has never been considered. Therefore a series of simulations have been performed to study the possibility for signal generation and the optimal conditions for its optical detection. Furthermore, model experiments have been conducted to verify and confirm that it is indeed possible to achieve detectable signal.

THERMAL BALANCE SIMULATIONS

Theoretically speaking, the specimen temperature should be locally risen by the electron beam irradiation and the heating effect should vanish shortly after the beam moves to another location. Therefore the process of signal extraction from this effect is very similar to the thermoreflectance problem [7, 8]. However the already conducted experiments usually employ light beams that are collimated or focused by objective lens from regular optical microscope. In the case of SEM the diameter of the electron beam is significantly smaller, so it is possible that the heating effect would be negligible and therefore impossible to measure. Furthermore there is a possibility that the material under examination is too inert (with respect to the heating modulation), which would cause dephasing of the induced thermal signal and the modulated incident beam, and additionally trouble the interpretation of the measured results.

All of the mentioned potential problems are prerequisites for conducting a more in-depth study of the

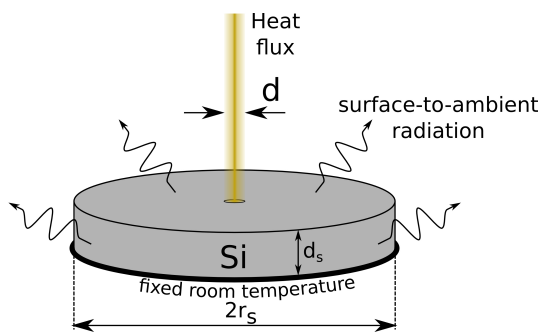


Fig. 1. Schematic representation of the set-up used for the simulations. A cylindrical Si-specimen with diameter $2r_s = 5$ mm and thickness $d_s = 1$ mm is heated by a beam (heat flux), with an integral energy of 90 mW, having Gaussian distribution of the energy. The beam diameter $d = 6\sigma$ may vary ($1 \mu\text{m} \leq d \leq 50 \mu\text{m}$). The bottom side of the specimen has constant temperature (293 K), whereas the other surfaces may cool down via surface-to-ambient radiation mechanism

electron-beam heating effect on micron scale. For this purpose a series of thermal balance simulations has been performed by specialised software – COMSOL Multiphysics. The simulated experimental setup is shown in Fig. 1: a cylindrical silicon specimen with diameter $2r_s = 5$ mm and thickness $d_s = 1$ mm is considered.

By means of the simulations, the heat transfer equation, Eq. (1), is solved (k stands for the material's thermal conductivity, and Q_i are all the heat sources (positive value) and heat sinks (negative sign) in W/m^3 units).

$$\rho C_P \frac{dT}{dt} - \nabla \cdot (k \nabla T) = \sum Q_i \quad (1)$$

To reach the desired solution some boundary conditions have been set. The bottom side of the cylindrical shaped sample has constant temperature of 293 K, which is also considered to be the initial temperature of the entire specimen. The rest of the surface is cooled by surface-to-ambient radiation, described by the following equation:

$$-\vec{n} \cdot (-k \nabla T) = \varepsilon \sigma_S (T_0^4 - T^4) \quad (2)$$

The left-hand side of this equation represents the heat flux through the specimen surface. Since the only considered in our model way for the specimen to cool down is radiation, the right-hand side of Eq. (2) is simply the Stefan-Boltzmann law, applied for grey body. In the discussed equation \vec{n} is normal vector to the specimen surface, k is the specimen's thermal conductivity, σ_S is the Stefan-Boltzmann constant and T_0 is the room temperature. The material's emissivity ε accounts for the deviation from the black-body radiation model.

Due to heating, the boundary condition for the top side is slightly more complicated.

$$-\vec{n} \cdot (-k \nabla T) = \varepsilon \sigma_S (T_0^4 - T^4) + P_0 G(r, \sigma) w(t) \quad (3)$$

Here a Gaussian-distribution $G(r, \sigma)$ of the energy is considered, the beam diameter is estimated by the standard deviation ($D = 6\sigma$). P_0 is the integral power of the heat source and $w(t)$ is a modulation function that simulates chopping of the heating beam. The nature of the energy flux source is not defined, so any result from these simulations apply for both heat sources: electron and laser beams. This is an important notice, as some of our experiments model the SEM heating effect by introducing a focused laser beam.

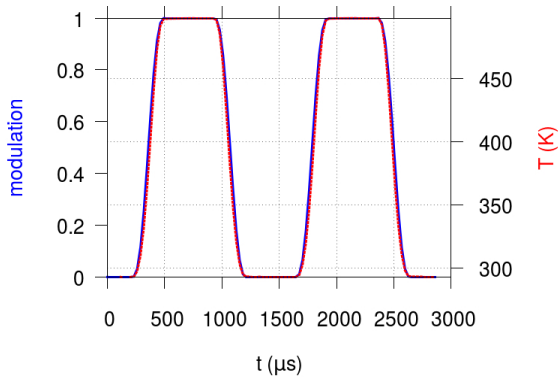


Fig. 2. Time dependences of the thermal (solid blue line) and the incident modulated signal (700 Hz, $d=5$ mm, 90 mW.) (dashed red line). Modulation is a (smoothed) square-wave signal that is used to chop the flux of the heat source. $T(k)$ is the temperature in the center of the heated area (measured on the specimen surface).

The simulations show that under typical conditions (beam diameter, integral heating power, modulation, etc.), the expected dephasing between the modulated incident and the induced thermal signals is negligible. Representative time dependences for incident 700 Hz modulated signal, with a beam diameter of 5 micrometers, and integral power of the heat source 90 mW, and that of the induced thermal signal are shown in Fig. 2. Simulations covered frequencies up to 1 kHz and no dephasing was observed even at the upper boundary. The results show the possibility of employing a thermoreflectance-like technique for material investigations.

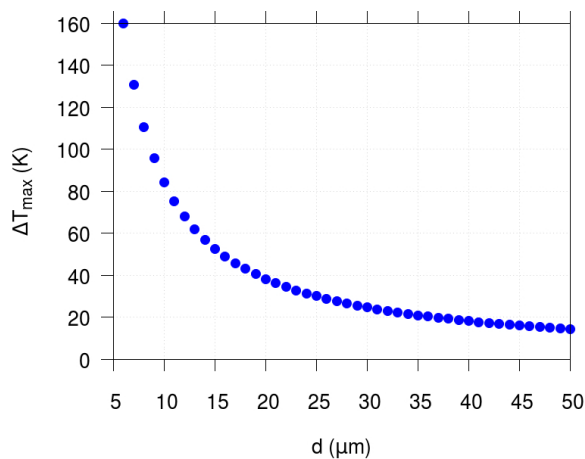


Fig. 3. Amplitude of the induced signal in the center of the heated area (see the red plot on Fig. 2), ΔT_{\max} , as function of the beam diameter d . The simulations are done for constant modulation frequency of 700 Hz and integral power of 90 mW of the incident beam.

The possible temperature amplitudes have also been simulated. A representative plot is shown in Fig. 3 where the incident beam modulation frequency of 700 Hz and 90 mW integral incident power were fixed and the beam diameter was varied. It is evident that with well focused beam it is possible to achieve relatively high temperature amplitudes. To ensure that such temperature changes are measurable a simple calculation was performed. For silicon the thermo-optic coefficient has order of magnitude $dn/dT \sim 10^{-4} \text{ K}^{-1}$ [12]. By means of an appropriate simulation, the relative changes in the reflection, R , at normal incidence, caused by infinitesimal refractive index alteration, could be estimated to be $(dR/dn)/R \sim 10^{-1}$. Therefore the relative reflection change, caused by temperature variations (see Fig. 3), is of the order of 10^{-5} K^{-1} , estimated by the following equation:

$$\frac{1}{R} \frac{dR}{dT} = \left(\frac{1}{R} \frac{dR}{dn} \right) \frac{dn}{dT} \quad (4)$$

Hence, if in the experimental set-up a lock-in amplifier with threshold $\left(\frac{\Delta R}{R}\right)_{\text{th}} \sim 10^{-6}$ is employed, the discussed relative variation of the reflectance, caused by the discussed temperature variations (see Fig. 3) can be considered detectable.

As stated above, the signal detection is optical – a probe beam is used to measure the changes in the materials reflection coefficient. Thus another concern raises – the heating effect could be focused in such a

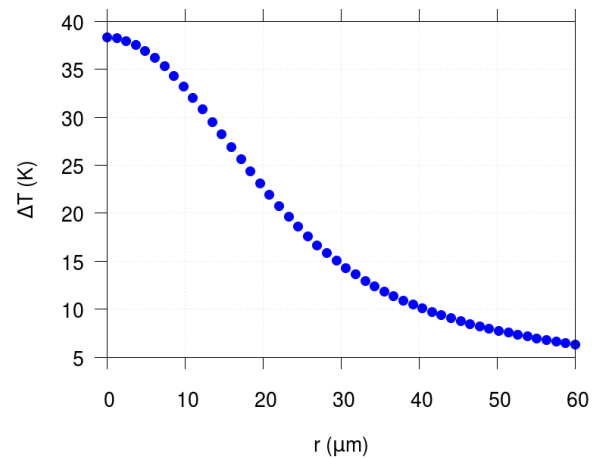


Fig. 4. Dependence of the induced thermal signal amplitude (see the red plot on Fig. 2), ΔT , on the radial distance from the beam (heat source) center. The incident beam has modulation frequency of 700 Hz, integral power 90 mW and 20 μm diameter.

tiny area, that it is much smaller than the field, illuminated by the probe beam. As already mentioned, the received signal is integrally averaged over the entire irradiated area, i.e. it is possible that the generated signal would be too weak for detection even with the used lock-in amplification methods. Therefore the radial distribution of the surface temperature of the specimen has also been examined. Fig. 4 shows the dependence of the induced thermal signal amplitude on the radial distance from the heating center (all data points are located on the specimen's top surface). Simulation results show that under these conditions the temperature amplitude is detectably high even at the distance of 60 μm . Our experience shows that with the use of standard optics a probe laser beam of about 200 microns in diameter can be achieved. Hence, the induced thermal signal, even localized around the incident beam, could be detected by means of optical methods.

OPTIMAL CONDITIONS FOR DETECTION OF THERMALLY-INDUCED ALTERATION OF THE REFRACTIVE INDEX

Even if one has achieved a measurable SEM beam heat effect, a lack of optimal experimental conditions could trouble the success of the experiments. Thus an important part of the current research is to define the optimal conditions for optical detection of the thermally-induced changes in the refractive index, i.e. to examine the sensitivity of the ellipsometric angles (ψ, Δ) with respect to the incident angle of the probe beam. The sensitivity of the reflection coefficients for both polarizations, R_p and R_s , having more general meaning, were also investigated, in order to find out whether optimal conditions exist, at which utilizing simple model experiments the general idea of the present work could be tested. Here, the theoretical optical response of a bulk material is simulated. For each of the four investigated parameters (ψ, Δ, R_p or R_s)

several steps are performed. Let F be any of those 4 parameters, then the simulation steps were as follows:

- Tabulation of F for discrete set of incidence angles, in the interval from 0° to 90° , with a step of 0.1° , assuming a constant refractive index;
- Alteration of the refractive index by $\Delta n = 0.001$ and subsequent tabulation of F_{alt} in the same interval as F ;
- as the thermo-optic coefficient dn/dT is relatively stable under constant external conditions, the sensitivity S , with respect to the angle of incidence, ϕ , can be evaluated by a derivative of type:

$$S(\phi) = \left(\frac{dF}{dT} \right)_\phi \approx \frac{dn}{dT} \frac{F_{\text{alt}}(\phi) - F(\phi)}{\Delta n} \quad (5)$$

In the simulations, three different types of materials were involved: with real refractive index (glass); with complex refractive index (gold and silver); system with complex refractive index of the substrate and a dielectric thin layer with known thickness, grown onto the substrate (SiO_2 layer applied onto a silicon substrate). Representative graphics for the last group are shown in Fig. 5. Based on the detailed analysis of the obtained results, the optimal values of the incident angle depending on the particular investigated optical parameter were defined (see Table 1).

MODEL EXPERIMENTS

The satisfactory simulation results were a strong motive for going further and conducting some simple model experiments. Their main purpose was to confirm the possibility to achieve optically detectable changes in the refractive index of a material, induced by heat source (beam), mimicking the SEM electron beam interaction with the specimens.

Initial experiments were performed with a set-up, which scheme is given in Fig. 6, where the heating effect is achieved by applying square-wave electrical pulses to the specimen (a 20 nm gold layer).

Table 1. Optimal angle of incidence, ϕ_{opt} , and polarization for investigation of different ellipsometric angles (ψ, Δ) and reflection coefficients (R_p, R_s) for different materials

Material	With regard to ψ, Δ	With regard to R_p, R_s	
Glass	$\phi_{\text{opt}} = 60^\circ$	$\phi_{\text{opt}} = 0^\circ$	s-polarization
Silver	$65^\circ \leq \phi_{\text{opt}} \leq 75^\circ$	$0^\circ \leq \phi_{\text{opt}} \leq 75^\circ$	both
Gold	$65^\circ \leq \phi_{\text{opt}} \leq 75^\circ$	$0^\circ \leq \phi_{\text{opt}} \leq 75^\circ$	both
Si / SiO_2 (5 nm)	$\phi_{\text{opt}} = 75^\circ$ (narrow interval)	$\phi_{\text{opt}} = 0^\circ$	s-polarization
Si / SiO_2 (180 nm)	$55^\circ \leq \phi_{\text{opt}} \leq 75^\circ$	$\phi_{\text{opt}} = 70^\circ$	both

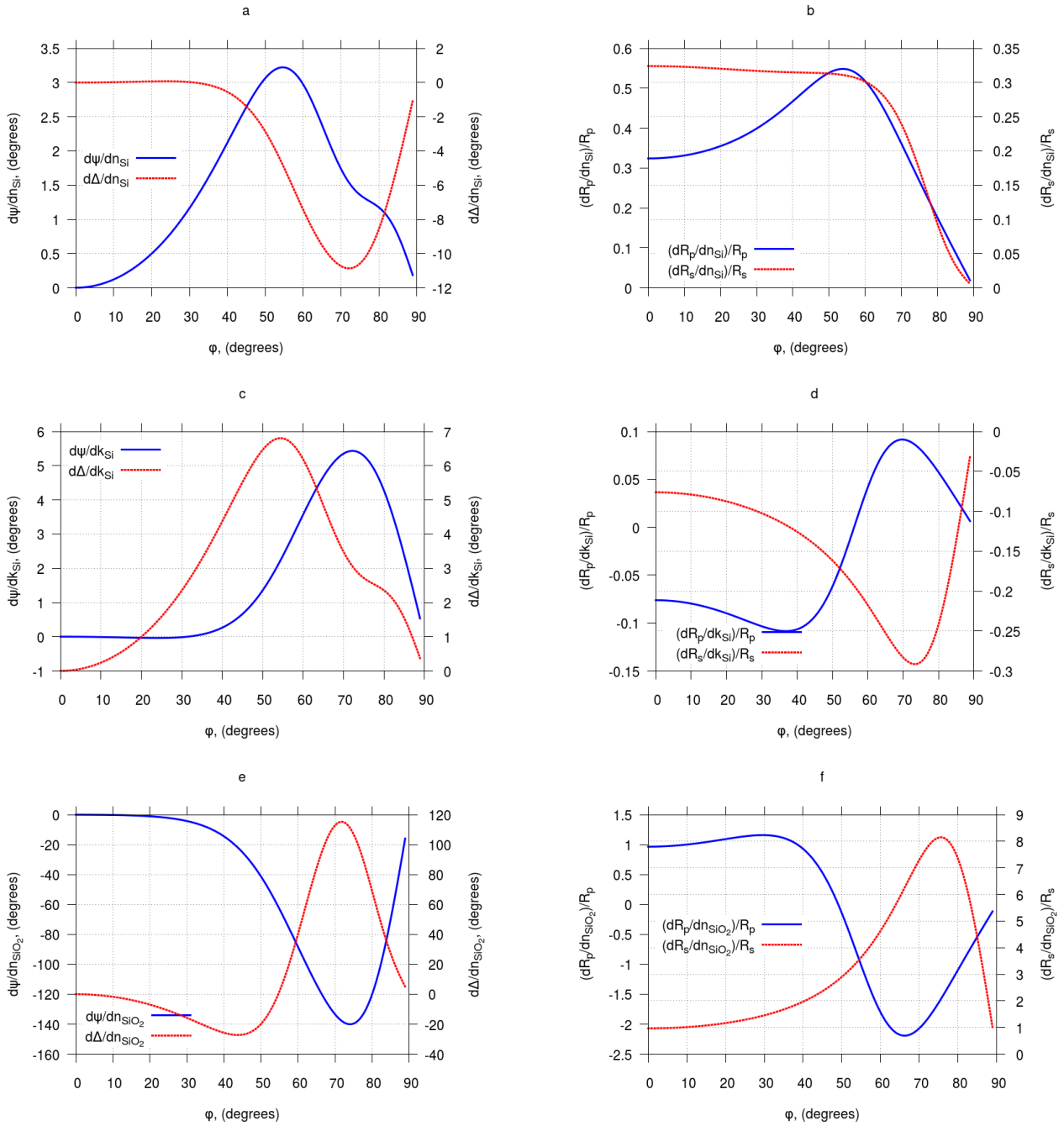


Fig. 5. Results (simulation) for a thin 180 nm SiO₂ layer, grown onto a Si substrate. Dependences on the angle of the beam incidence, ϕ , of the optical response of the system with respect to different ellipsometric and optical parameters: **a)** The optical response $d\psi/dn$ and $d\Delta/dn$ where ψ and Δ are the ellipsometric angles and dn is infinitesimal change in the real part of the refractive index of Si. The complex part, k , as well as the refractive index of SiO₂ are considered constant; **b)** the optical response with respect to the more general parameters, the reflection coefficients R_p and R_s (same conditions as a.); **c)** $d\psi/dk$ and $d\Delta/dk$, where the complex part of the Si refractive index is varied (constant real part and SiO₂ refractive index); **d)** Optical response with respect to R_p and R_s under the same conditions as c.; **e)** $d\psi/dn$ and $d\Delta/dn$, when the refractive index of SiO₂ is varied and that of the silicon remains constant; **f)** Optical response of the system with respect to R_p and R_s (same conditions as e.).

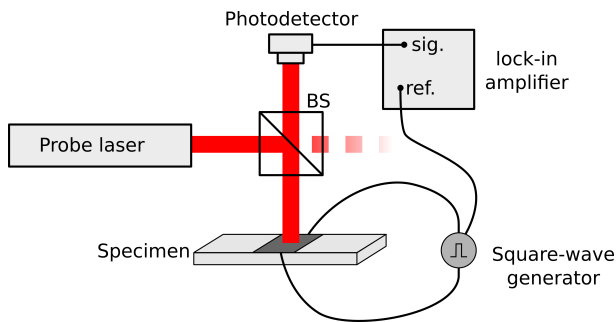


Fig. 6. Set-up for the electrically heating sample experiment. A 20 nm thick gold film(specimen) was heated by square-wave current pulses with chosen frequency and duty cycle (heating power is approximately 1.3 W). A 658 nm semiconductor laser provided the probe beam. A lock-in amplifier was used to analyze the signal. The photodetector used was Thorlabs PDA36A.

Refractive index changes were detected by continuous monitoring the intensity of a normally reflected probe beam. The pulse frequency and duty cycle could be controlled by the operator. Synchronizing pulses were also fed from the generator to the lock-in amplifier, which analyses the signal and measures its amplitude at low signal-to-noise ratio. Due to insufficient isolation from external noises, good reproducibility of the experiments was not achieved, but our observations made it evident that variation of the

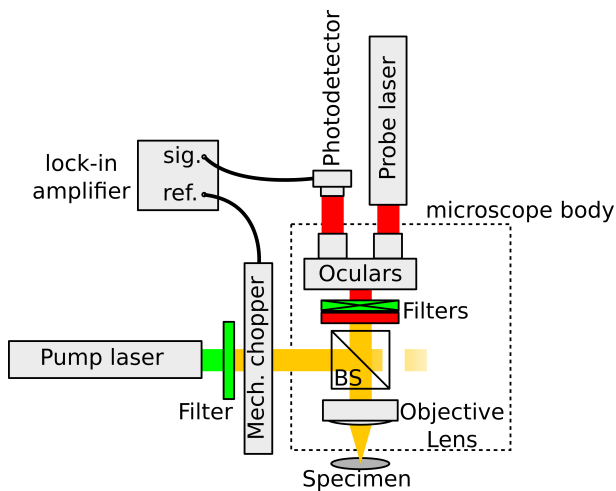


Fig. 7. Set-up for the laser heating experiment. A pump laser (532 nm) is focused on the specimen, providing the heating effect. Incident beam modulation (723 Hz, 50% duty cycle) is achieved by mechanical chopper. The probe laser (658 nm) passes through the oculars and the objective lens, then reflects normally. The photodetector used was Thorlabs PDA36A. Both laser beams are spectrally isolated.

pulse amplitude changed the indication of the lock-in amplifier, i.e. a desired sensitivity of the method existed. We believe that the generated thermal signal could be measured, provided that the external noises are eliminated.

Apart from the expected optical signal, also acoustic wave generation was detected. Surprisingly, the sound was loud enough to be heard by the operator in a silent laboratory, i.e. the acoustic signal seemed to be much more intense than the optical one. However, future use of this side effect is yet to be discussed, since the sound waves, which were generated in our experiment in air, have to be detected in appropriate manner, since the experiments in SEM chamber are carried out under vacuum. Similar results have been obtained before, and an entire experimental technique has been developed, known as SEAM [11].

A second series of experiment was also conducted. The experimental set-up (Fig. 7) was built to better resemble the real experimental conditions. As heat source, a laser beam (semiconductor laser with wavelength of 658 nm) was used, which modulation was achieved by mechanical chopper. For more stable and easily constructed assembly, a standard optical microscope was used. Its objective lenses focus both the probe and the pump laser beams on the specimen surface. To spectrally isolate the beams colour filters were used.

The probe laser beam passes through one of the oculars, and then normally reflected beam (from the specimen surface) reaches the photodetector, mounted into the other ocular. The signal is once again analyzed by a lock-in amplifier. A total of two materials were examined: silicon and indium phosphide plates. The obtained initial results are shown in Table 2. Despite the small amount of conducted experiments, a good data reproducibility under constant conditions was observed. However, there were

Table 2. Experimental values of relative reflection coefficient, $\Delta R/R$, with respect to the gain, B, of the photodetector, for two different samples, obtained by the set-up, shown in Fig. 7

Specimen	$(\Delta R/R) \times 10^6$	B, dB
Si	25	60
InP	10	50
InP	7	50
InP	20	60
InP	16	60

still external noise sources present, e.g. the vibrations of the mechanical chopper. An interesting observation was the non-linearity of the gathered signal – although the relative reflection coefficient changes were measured ($\Delta R/R$), different gain levels of the detector's pre-amplifier yielded different signal amplitudes (see Table 2). This result is still to be investigated, since the DC signal levels were well below the detector's saturation cap in all measurements.

CONCLUSIONS

In general, heating effect and/or carrier injection induced by accelerated electrons, result in material refractive index variation. The possibility to detect such alterations by means of optical methods and in particular with ellipsometry, was investigated. A series of simulations has been performed, and the results confirmed that detectable signal could be generated, when a heat effect appeared in a sample, heated by a beam (heat source). Another series of simulations helped one to find the optimal condition for signal detection. Based on these results, two simple set-ups were built up and model experiments were conducted. The experimental results confirm in general, the sensitivity of the reflection coefficient to the induced, by the heat, local optical properties changes. Thus it is noteworthy to continue the research with new, more realistic experiments, e.g. measuring the optical response under high vacuum and moving on to determine the ellipsometric angles instead of reflection coefficient.

REFERENCES

- [1] H. Fujiwara, *Spectroscopic Ellipsometry: Principles and Applications*, Wiley (2007).
- [2] R.M.A. Azzam, N.M. Bashara, *Ellipsometry and polarized light*, North-Holland personal library, North-Holland Pub. Co. (1977).
- [3] R. Egerton, *Physical Principles of Electron Microscopy: An Introduction to TEM, SEM, and AEM*, Springer (2006).
- [4] D. Bouscaud, R. Pesci, S. Berveiller, E. Pattoor, *Ultramicroscopy* **115**, 115–119 (2012); <http://dx.doi.org/10.1016/j.ultramic.2012.01.018>
- [5] M. Liu, L. Xu, X. Lin, *Scanning* **16**, 1–5 (1994); <http://dx.doi.org/10.1002/sca.4950160102>
- [6] J. A. Morrison, S. P. Morgan, *Bell System Technical Journal* **45**, 661–687 (1966); <http://dx.doi.org/10.1002/j.1538-7305.1966.tb01051.x>
- [7] D. G. Cahill, P. V. Braun, G. Chen, D. R. Clarke, S. Fan, K. E. Goodson, P. Keblinski, W. P. King, G. D. Mahan, A. Majumdar, H. J. Maris, S. R. Phillpot, E. Pop, L. Shi, *Appl. Phys. Rev.* **1**, 1–45 (2014); <http://dx.doi.org/10.1063/1.4832615>
- [8] A. J. Schmidt, R. Cheaito, M. Chiesa, *Rev. Sci. Instrum.* **80**, 1–6 (2009); <http://dx.doi.org/10.1063/1.3212673>
- [9] C. R. Brundle, C. A. Evans, S. Wilson, *Encyclopedia of Materials Characterization: Surfaces, Interfaces, Thin Films*, Characterization Series, Butterworth-Heinemann (1992).
- [10] J. Misiewicz, P. Sitarek, G. Sek, *Opto-Electron. Rev.* **8**, 1–24 (2000).
- [11] D. G. Davies, R. E. Green, M. Somekh, G. Busse, *Philos. Trans. R. Soc. London, Ser. A* **320**, 243–255 (1986).
- [12] B. J. Frey, D. B. Leviton, T. J. Madison, *Proc. SPIE* **6273**, 62732J–62732J-10, (2006); <http://dx.doi.org/10.1117/12.672850>

ЕЛИПСОМЕТРИЧНА ДЕТЕКЦИЯ НА ОПТИЧНО И ЕЛЕКТРОННО-ЛЪЧЕВО ИНДУЦИРАНО
ИЗМЕНЕНИЕ НА ОПТИЧНИТЕ СВОЙСТВА НА МАТЕРИАЛИ И СТРУКТУРИ

Ст. Хаджийски, Д. Лютов, К. Кирилов, К. Генков, Г. Цуцуманова, А. Цонев, Ст. Русев

*Физически факултет, Софийски университет "Св. Климент Охридски",
ул. „Джеймс Баучер“ №5, 1164 София, България*

(Резюме)

Целта на тази работа е предварително изследване на възможността за съчетаване на предимствата на две различни експериментални техники – елипсометрия и сканираща електронна микроскопия (СЕМ). Елипсометрията е добре развит безконтактен и безразрушителен метод с много добра чувствителност по отношение на изменение на оптичните свойства и/или геометрията, перпендикулярно на интерфейса, но има ограничена разделителна способност в равнината. От друга страна СЕМ предлага много по-добра разделителна способност, като обикновено детектирания сигнал са вторични или обратно разсеяни електрони, фотони (катодолуминесценция) или рентгеново лъчение (EDX). В допълнение, взаимодействието на електронния лъч с повърхността на образеца води до локално изменение на температурата и до инжекция на токоносители. Това от своя страна изменя локално показателя на пречупване и може да бъде детектирано по принцип елипсометрично, давайки възможност за визуализация на термичните свойства с микронна разделителна способност.

Проведени са редица симулации за изучаване на електронно-лъчевото загряване в СЕМ и са изследвани оптималните условия за оптична детекция. Поставени са и моделни експерименти, потвърждаващи получените от симулациите данни.